A Net-Zero Carbon Supply Chain Model: Minimizing the Cost of Onsite Renewable Energy

Tongdan Jin[1,1], An Pham[1], Clara Novoa[1], Cecilia Temponi[2]

[1]Ingram School of Engineering, Texas State University, San Marcos, TX 78666, USA
[2]McColy College of Business, Texas State University, San Marcos, TX 78666, USA
{tj17@txstate.edu, a_p276@txstate.edu, cn17@txstate.edu, ct01@txstate.edu}

Abstract. This paper analyzes whether it is feasible to deploy and operate a net-zero carbon supply chain via onsite wind and solar generation. A linear programming model is formulated to determine the sizing and siting of renewable power units in an integrated production-transportation system with the goal of minimizing the levelized cost of energy. Numerical experiments show that it is technically feasible and financially affordable to operate a zero-carbon supply chain provided the local facility possesses a medium wind speed and the equipment cost of PV drops to $2 per watt.

Keywords: Zero-carbon supply chain design, logistics electrification, linear programming

1 Introduction

It is estimated that the manufacturing industries consume 30-40 percent of the total electricity used in the world. Electric energy is used primarily for powering the machines and tooling equipment, the heating ventilation & air conditioning, office lighting, and other critical production processes. For instance, a semiconductor wafer manufacturing facility operating 24 hours a day, 7 days a week has an average power consumption of 15-30 MW [1]. Since the large portion of grid electricity is generated by burning fossil fuels (i.e. coal, oil and natural gas), this is equivalent to releasing 91,000 to 180,000 tons of carbon each year. Also, electricity cost of a wafer fab is as high as $20-30 million/year.

Road transport is another large contributor to greenhouse gases (GHG) emissions, representing 27% of the total emissions in 2011 [2]. In North America there are more than 15.5 million trucks, of which 2 million are tractor trailers, running on the continental roads [3]. As a result, the US trucking industry consumes 52.3 billion gallons of fuel per annum, accounting for 12.8% of all the fuel purchase in the nation. In 2011 the transportation industry in North America logged 432.9 billion miles (1 mile=1.6 km), which is equivalent to circling the equator 17,316 times. Based on a new report released by American Trucking Associations, it is projected that freight volumes and the truck fleet will increase by nearly 29% over the next decade due to the growth of population and the rapid development of emerging markets. Hence, reducing the transport carbon footprint becomes a grave concern of truck manufacturers, logistics companies and policy makers around the world.

Driven by the concern of climate change, firms are striving to attain sustainable operations by directly integrating onsite renewable energy into their business processes. For instance, by 2013 retail giant Walmart had more than 335 world-wide renewable energy projects, mainly onsite solar photovoltaics (PV) systems [4]. Two major obstacles against the large-scale adoption of onsite wind and solar are the power intermittency and the equipment cost. Energy storage such as pumped hydro storage system can be used to absorb excessive wind and solar power [5], yet the high upfront investment of today's storage systems precludes their broad implementation in an enterprise.

This paper proposes an onsite grid-connected wind and solar generation system to power a multi-echelon supply chain system comprised of production, warehousing, retailing and transportation functions. Benjaarfar et al. [6] discuss various renewables incentives such as carbon tax, carbon trading and carbon cap, and their impacts on supply chain designs. Chen and Chiu [7] present a case-based analytic method for a sustainable supply chain network design considering customer, environmental and social values. Villarreal et al. [1] propose to use on-site wind and solar energy for powering wafer fabs, yet their study focuses on a single facility without considering transportation and warehousing.

[1] This research is partially supported by The USDA (grant #: 2011-38422-30803).

This paper aims to determine the generation type and capacity for a supply chain such that the levelized cost of renewable energy is minimized. "Levelized energy cost" is the metric to measure the expense of producing one MWh (Megawatt-hour) of electricity given different generation technologies [8]. The contribution of the paper is twofold. First, we take an early step to perform an eco-economic analysis of onsite renewable technology in a multi-facility environment. Second, we develop a quantitative model that can guide firms to assess the intermittent power sources for attaining carbon-free supply chain performance.

Section 2 addresses issues associated with integration of onsite renewables in supply chain. Section 3 models the zero carbon operations for a multi-location supply chain. Section 4 presents the numerical experiments. Section 5 provides conclusions and future research.

2 Integrating Onsite Renewables in Supply Chains

2.1 Carbon Emissions vs. Savings

Table 1 presents the carbon footprint for different entities (i.e. human being, gasoline cars, battery electric vehicles (BEV), residential homes, manufacturing facilities and data centers) and the carbon saving realized by WT and solar PV. Emission metrics are calculated based on the fact that the carbon intensity rate is 0.6-0.9 kg CO_2 per KWh depending on whether gas, oil or coal is burned in power plants [9]. Obviously, the largest carbon contributors are manufacturing facilities and data centers. Though a BEV has no tail-pipe emissions, if the battery is charged by the conventional grid, the emission rate is only 18% lower than the gasoline cars.

Table 1: Annual Carbon Emission vs. Saving (MW= megawatt, KWh=kilowatt-hour)

Entity	Basic Fact	Emissions (tons)	Savings (tons)
Human Being	~ 1 kg/person/day	0.365	
Gasoline Car*	0.3 kg/mile	3.60	
PEV/EV*	35 KWh/100 miles	2.94	
Single Family	48-96 KWh/day	10-20	
Manufacturing Facility	15-30 MW	92-184x10^3	
Large Data Center	40-50 MW	298x10^3	
Wind Turbine**	1-3 MW		2.5-7.4x10^3
Solar PV***	0.5-1 MW		0.55-1.1x10^3

Note: *based on 12,000 miles/year, **capacity factor is 0.4, and *** capacity factor is 0.35

2.2 Network Architecture

As shown in Figure 1, the supply chain we study consists of multiple plants, warehouses and retail stores. Each facility is powered by an onsite generation system comprised of wind turbine (WT) and photovoltaics (PV) systems. We assume that the distance between two adjacent facilities is large enough so that wind profiles and weather conditions are uncorrelated.

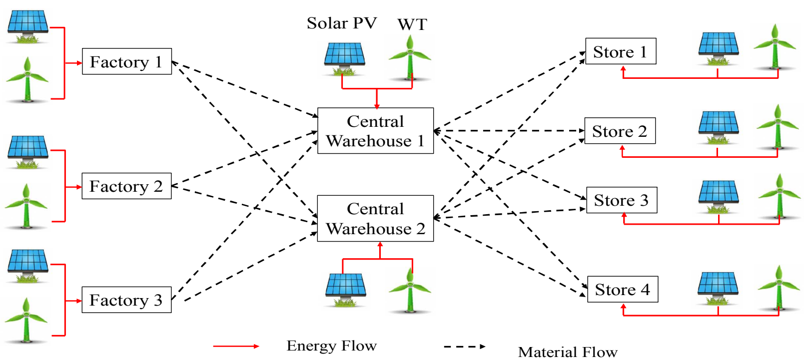

Figure 1: A Multi-Echelon Supply Chain with Onsite Renewable Generation

Ensuring reliable supply of wind and solar energy is the first priority to design this type of Distributed Generation (DG) system. Two options are generally available: 1) fully islanding mode (i.e. microgrid); and 2) grid-connected onsite generation. In the former, the onsite energy system is disconnected of the main grid. However, such an islanding operation is technically challenging given the intermittent output of WT and PV units. Therefore, this paper proposes to use a grid-connected DG system to power the facility. If the output of the local DG system is less than the load, the shortage can be filled by importing the electricity from the main grid. If surplus energy is produced from the DG, it can be fed into the main grid via net metering. For a supply chain, net-zero carbon emissions are achieved whenever the energy imported from the main grid is counter-balanced by the renewable energy fed into the grid during the course of a year. Figure 2 shows the working principle of a grid-connected DG system at one factory. Similar architecture can be applied to the central warehouses and the retail stores.

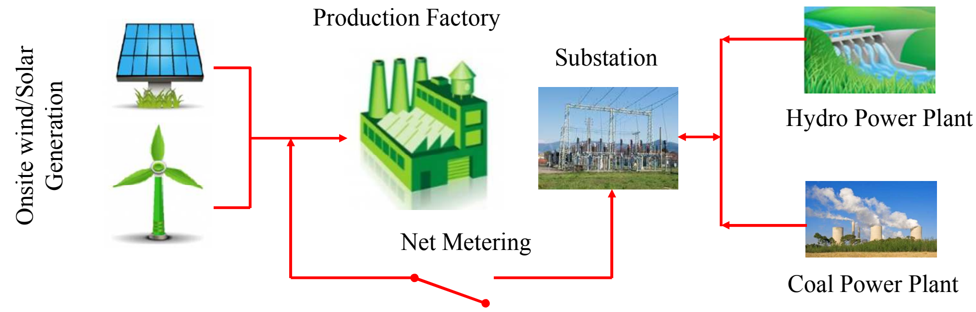

Figure 2: A Grid-Connected Onsite Generation System

2.3 Modeling Wind Generation

The cubic function is commonly used to estimate the instantaneous power output of a WT unit. Define v_c as the cut-in speed, v_r as the rated speed, and v_s as the cut-off speed, respectively. Let $P_w(y)$ be the WT output power at wind speed y at any time, then

$$P_w(y)=\begin{cases} 0 & 0<y<v_c, or\ y>v_s \\ \gamma y^3 & v_c \le y \le v_r \\ P_m & v_r \le y \le v_s, \end{cases} \tag{1}$$

where, P_m is the rated power or the capacity of a WT unit, and $\gamma=P_m/v_r^3$. The capacity factor of a generating unit is the ratio of its actual output energy over a period of time T to its potential output if operating at fully rated capacity. Based on equation (1), the capacity factor for a WT unit, denoted as λ_w can be estimated as

$$\lambda_w=\frac{E[P_w(y)]\times T}{P_m \times T}=\frac{1}{v_r^3}\int_{v_c}^{v_r} y^3 f_w(y)dy+\left(F_w(v_s)-F_w(v_r)\right), \tag{2}$$

where $f_w(y)$ and $F_w(y)$ are, respectively, the probability density function and the cumulative distribution function of the random wind speed Y. The value of λ_w is in the range $[0, 1]$.

2.4 Modeling Solar PV Generation

Let S be the random variable representing the solar irradiance incident on the PV surface at time t, and s be the realization. The solar irradiance is usually measured in W/m^2. The output power of a PV panel, $P_{pv}(S)$, depends on multiple factors, including weather condition, daily hour, calendar date, panel size, orientation, tilt angle, efficiency, and operating temperature, among others. Originally proposed by Cai et al. [10], a generic PV model incorporating weather uncertainty is given as.

$$P_{pv}(S)=\eta AS(1-0.005(T_o-25)), \tag{3}$$

In (3), η is the PV efficiency, A is the panel area (in m^2), and T_o is the PV operating temperature (^oC). Under clear sky condition, the hourly PV generation can be precisely predicted at any time t. Similarly, the capacity factor for a PV system is given by

$$\lambda_{pv} = \frac{E[P_{pv}(S)]\times T}{P_{pv}(s_m)\times T} = \frac{(1-0.005(T_o-25))\int_0^{s_{\max}} xf_S(x)dx}{s_{\max}}, \tag{4}$$

where $s_{\max}$ is the largest solar irradiance received by the PV panel during the course of a year, and $f_S(x)$ is the probability density function for S. The probability distribution of S can be deduced from the historical solar radiation data.

3 Battery Recharging and Transport Electrification

3.1 Battery Recharging Technologies

The first Direct Current (DC) charging standard is the Japanese CHAdeMO which combines Alternating Current (AC) and DC charging in a single connector/inlet. Hence, it requires two separate connectors/inlets, one for AC and one for DC. Later, the U.S. Society of Automotive Engineers (SAE) propose the SAE J1772 standard to regulate the EV charging process by covering the connector and charging cable based on 120V and 240V [11]. The SAE J1772 is a commercial standard Coupler for all DC faster chargers. It can be used in the public charging station. SAE J1772 also developed a Combo Coupler variant of the J1772-2009 connector with additional pins to accommodate fast DC charging at 200–450V and up to 90kW. The SAE J1772-2009 has been adopted by the car manufacturers, and used in the third generation of the Chevrolet Volt and Nissan Leaf as the early models.

The charging level is determined by the voltage and current, or specifically the electric power. Three different charging levels have been defined, but other options are available to accommodate the diversity of existing power grid standards of the national electricity generating utilities. Table 2 sows the different charging levels, its voltage, current and power characteristics as well as the estimated time to charge. Due to the higher recharger times of Level I, it is used in residential areas. Typical charging time in Level I is 12 hours or could be longer and up to 18 hours. It is suitable for overnight home charging. The Level II and Level III are often used in the public charging station. Level 2 could be also implemented in homes where the last mile electric distribution line voltage is 220V, which is common in Europe and China. Level III, a fast charging mode, has a high voltage and high-current charging implementation. For example, a Level 3 charger allows a Nissan Leaf's battery to be charged to its 80% capacity in 30 minutes (the battery capacity is 24KWh).

Table 2: Three Levels of Battery Recharging Technologies

Level	Location	Voltage and Current	Power (KW)	Estimated Time to Charge
I	Residential	110V, 15 A	1.4	12-18 hours
II	Residential/ Public	220V, 15-30 A	3.3	4-8 hours
III	Commercial	480V, 167 A	50-70	20-50 minutes

3.2 Electric Transport Energy Intensity Rate

The electric energy required to move an object from one location to another depends on the mass of the object, the distance traveled, and the speed. For example, according to Nissan [12], the battery capacity of a Nissan Leaf is 24 KWh, and the maximum drive range of a fully charged Leaf can reach up to 70 miles (i.e. 112 km) at the speed of 100 km/hour. The gross vehicle weight of the Leaf is 1,800 Kg (including passengers); this implies the electric transportation intensity rate is

$$q = \frac{24}{112\times 1800} = 1.19\times 10^{-4}\ KWh/kg/km. \tag{5}$$

Equation (5) indicates that the amount of electricity required to move a 1-Kg object for 1 km at 100km/hour is 1.19×10^{-4} KWh. If we want to move a 4,000-kg object over 100 km at a speed of 100 km/hour, the amount of electricity consumed would be $q\times4000\times100=47.62$ kWh (note 1000 KWh=1 MWh).

4. Zero Carbon Operations for a Multi-Location Supply Chain

4.1 Annualized Energy Cost

Let i be the index for the facility and j the index for the electricity generation technology. Let $\overline{D}_i$ be the average electricity demand (MW) in facility i, and P_{ij}^c be the capacity of generation type j at facility i. In addition, let B_i be a variable whose value depends or is a function of the power generated by wind and PV technologies at location i. The value of B_i is positive if the demand exceeds the sum of wind power and PV, and negative otherwise. Thus B_i is given by the following equation.

$$B_i = \overline{D}_i - \sum_{j=1}^{J} \lambda_{ij} P_{ij}^c, \qquad \text{for } i=1, 2, \ldots, I. \tag{6}$$

where λ_{ij} is the capacity factor for generation type j at facility i. Since B_i is unrestricted in sign, it can be written as the subtraction of two non-negative variables as follows

$$B_i = B_i^{'} - B_i^{"}, \qquad \text{for } i=1, 2, \ldots, I. \tag{7}$$

In equation (7), $B_i^{'}$ represents the energy imported from the main grid to a particular facility i when the demand exceeds the total energy from wind power and PV. On the other hand, $B_i^{"}$ represents the surplus energy produced from WT and PV that is fed into the main grid via net metering. Upon operating the DG system over a year, if $B_i^{'}$ ends positive then $B_i^{"}$ is zero, and vice versa. On a supply chain with net-zero carbon emissions, the electric energy imported from the main grid is counter-balanced by the renewable energy fed into the grid during the course of a year. It can be stated that ideally $\sum_{i=1}^{I} B_i = 0$ holds true.

The aggregate cost of the onsite DG system consisting of installation, operations and maintenance (O&M), carbon credits, and net metering is given by

$$C_{DG}=\phi\sum_{i=1}^{I}\sum_{j=1}^{J}a_j P_{ij}^c+\tau\sum_{i=1}^{I}\sum_{j=1}^{J}b_{ij}\lambda_{ij}P_{ij}^c-\tau\sum_{i=1}^{I}\sum_{j=1}^{J}c_{ij}\lambda_{ij}P_{ij}^c+\tau\sum_{i=1}^{I}\rho_i B_i^{'}-\tau\sum_{i=1}^{I}\delta_i B_i^{"}, \tag{8}$$

In equation (8), the first term represents the annualized equipment cost. The capital recovery factor, ϕ, is given by $\phi = [r(1+r)^n]/[(1+r)^n - 1]$ where n is the number of years to pay the equipment loan, and r is the interest rate. The parameter a_j is the capacity cost of generation type j in \$/MW, and P_{ij}^c is the capacity of generation type j in location i. The second term captures the O&M cost of the generating units. Note that τ is the number of hours in a year and b_{ij} is the O&M cost in \$/MW for generation type j at facility i. In the third term, c_{ij} represents the carbon tax credits awarded to generation type j at facility i and it is in \$/MW. The last two terms capture the net metering through the use of the $B_i^{'}$ and $B_i^{"}$ variables discussed in equation (7). The parameter ρ_i is the electricity purchasing cost (\$/MWh) at facility i and δ_i is the feed-in tariff (\$/MWh) of returning extra renewable energy to the main grid at facility i.

This paper focuses on a net-zero carbon emission case where the electricity purchasing cost ρ_i and the feed-in tariff δ_i for each i^{th} facility are assumed equal and consequently the last two terms in equation (8) vanish.

4.2 Transportation/Logistics Energy

To achieve zero carbon transportation, our model employs battery-powered freight vehicle fleets to ship finished goods from the factories to the warehouses and further to the local stores. Let d_{ik} for $i\neq k$ be the distance between an upstream and a downstream facility. Distance $d_{ik}=0$ if there is no direct route between i and k with i and k=1, 2, …, I (see Figure 1). The annual transportation energy (KWh) across the entire supply chain network can be estimated as

$$E_{TR} = q\sum_{i=1}^{I}\sum_{k=1}^{I} n_{ik} d_{ik}(w_{ik}^{p} + w_{ik}^{v}) + q\sum_{i=1}^{I}\sum_{k=1}^{I} n_{ik} d_{ik} w_{ik}^{v}, \tag{9}$$

where, q is the electric transport energy intensity rate which is computed as discussed previously in equation (5), n_{ik} be the number of yearly trips between locations i and k. In addition, w_{ik}^{p} and w_{ik}^{v} are, respectively, the payload and the vehicle self-weight per trip between locations i and k. The first term in equation (9) captures the annual electric energy required for charging the vehicle batteries to ship the goods from factories to central warehouses and further down to stores. The second term captures the annual electricity consumed when the e-freight vehicles travel from stores to warehouses, and further up to the factories (i.e. in the reverse direction). Since vehicles travel unloaded in the reverse direction, less electric energy is consumed.

4.3 Minimizing Levelized Cost of Energy

Our goal is to minimize the levelized cost of energy (LCOE) of the supply chain subject to net-zero carbon emission constraint. LCOE is defined as the aggregated energy cost divided by the cumulative renewable energy generation in a year. Denoted as Model P1, the DG optimization problem can be formulated as a linear programming model as follows

Model P1:
Minimize:

$$f(\mathrm{P}^{c}) = \frac{1}{E_{TR} + \tau\sum_{i=1}^{I}\overline{D}_{i}}\left(\phi\sum_{i=1}^{I}\sum_{j=1}^{J} a_{j} P_{ij}^{c} + \tau\sum_{i=1}^{I}\sum_{j=1}^{J} b_{ij}\lambda_{ij} P_{ij}^{c} - \tau\sum_{i=1}^{I}\sum_{j=1}^{J} c_{ij}\lambda_{ij} P_{ij}^{c}\right), \tag{10}$$

Subject to:

$$\tau\overline{D}_{i} + q\sum_{k=1}^{I} n_{ik} d_{ik}(w_{ik}^{p} + w_{ik}^{v}) + q\sum_{k=1}^{I} n_{ik} d_{ik} w_{ik}^{v} = \tau\sum_{j=1}^{J}\lambda_{ij} P_{ij}^{c}, \text{ for } i=1, 2, \ldots, I \tag{11}$$

$$P_{11}^{c}, P_{12}^{c}, \ldots P_{ij}^{c} \ldots, P_{IJ}^{c} \geq 0. \tag{12}$$

$\mathbf{P}^{c}=\{P_{11}^{c}, P_{12}^{c}, \ldots, P_{ij}^{c} \ldots, P_{IJ}^{c}\}$ are the decision variables representing the power capacity of generation type j to be allocated at location i. The objective function (10) minimizes the LCOE. The numerator captures the annualized generation cost and the denominator is the expected energy demand in a year. E_{TR} represents the annual energy needed for battery recharging given in equation (9). Constraint (11) prescribes that the energy output in location i shall be equal to the total electricity consumed by the facility and the electric vehicles. Constraint (12) states that all the decision variables are non-negative. Since Model P1 is a linear programming model, off-the-shelf solvers can search for its optimal solution.

5. Numerical Experiments

We construct a numerical example based on the supply chain network in Figure 1 where the total number of facilities I=9, with i=1, 2, 3 being the index for factories, i=4 and 5 for central warehouse, and i=6, 7, 8, 9 for retail stores. Data associated with WT and PV is in Table 3.

The lifetime of WT and PV is n=20 years, and the loan interest rate r=5%. In this example, we have J=2, with j=1 for WT, and j=2 for PV. The units for power and energy are MW and MWh, respectively (note: 1 MW=10^3 KW=10^6 W, and 1 MWh=10^3 KWh=10^6 Wh). The electric transportation intensity rate q=1.19×10^{-7} MWh/kg/km. A homogenous vehicle fleet is employed for shipping goods between facilities. The self-weight of the vehicle is w_{ik}^{v}=7,000 kg. The electricity demand for the three factories is D_1=D_2=D_3=12 MW, for the two warehouses is D_4=D_5=8 MW, and for the retail stores is D_6=D_7= D_8=D_9=4 MW. These values may vary with the actual applications, yet they are appropriately chosen to reflect the typical energy usage in a production-transportation network. Other parameters relevant to the transportation model are given in Tables 4 and 5.

Table 3: WT and PV Equipment, Operation, Maintenance and Carbon Credits

Symbol	Wind Turbine			Symbol	Solar PV		
a_j	Capacity cost	1.5×10^6	\$/MW	a_j	Capacity cost	4×10^6	\$/MW
b_{ij}	O&M cost	14	\$/MWh	b_{ij}	O&M cost	8	\$/MWh
c_{ij}	Carbon credits	0	\$/MWh	c_{ij}	Carbon credits	35	\$/MWh
τ	Operating hours	8760	hours/year	τ	Operating hours	8760	hours/year
v_c	Cut-in speed	2	m/s	η	Efficiency	0.15	N/A
v_r	Rated speed	10	m/s	T_o	Operating Temperature	45	^{o}C
v_s	Cut-off speed	25	m/s	n	Load period	20	years

We compute the LCOE of the supply chain under different climate conditions in the facilities. The WT capacity factors (CF) are classified into three categories, high (H), medium (M), and low (L), with H=0.4, M=0.3 and L=0.2. Similarly, PV CF are classified into three categories with H=0.3, M=0.2 and L=0.1. Case 1 (see Table 6) is the baseline and corresponds to the state in which the CFs for WT and PV are in the high level. We solve Model P1 and the LCOE is \$48.35/MWh. It is also found that given a \$35/MWh carbon credit to PV, WT is still more competitive than PV. Hence the resulting aggregate installed capacity of WT in nine locations is 170.4 MW. The climate condition in Case 2 is opposite to Case 1 with low wind speed and solar irradiance across the network. Though WT turns to be more cost effective than PV, the LCOE is \$82.7MWh, which is 71% higher than that in Case 1. In Case 3, we assume all facilities have a low wind profile, yet high solar radiation. To our surprise, WT is still a cost-effective energy solution against PV.

Table 4: Transportation between Factory and Central Warehouse (CW)

	Distance (km)		Frequency per Year		Goods per vehicle (kg)	
	CW 1	CW 2	CW 1	CW 2	CW 1	CW 2
Factory 1	100	150	180	150	18000	15000
Factory 2	120	160	200	250	2000	25000
Factory 3	90	140	130	330	13000	33000

Table 5: Transportation between Central Warehouse and Retail Store (RS)

	Distance (km)				Frequency per Year				Goods per vehicle (kg)			
	RS1	RS2	RS3	RS4	RS1	RS2	RS3	RS4	RS1	RS2	RS3	RS4
CW 1	150	200	250	300	80	40	50	30	20000	15000	8000	2500
CW 2	80	100	130	170	50	60	30	45	6500	5000	12000	14000

In Case 4, we keep the same climate condition as in Case 3, yet reduce the capacity cost of PV in 50%. It is interesting to see that PV becomes more completive than WT. In Case 5, we assume all facilities have high wind and solar radiation, and we look to identify at what capacity cost level PV can compete with WT. We found that when the PV capacity cost goes down to \$$10^6$/MW, PV can compete with WT in terms of LCOE. In Case 6, we assume that factories have high wind profiles while CW and RS possess low wind speed. Our optimization program shows that PV is more favorable in CW and RS provided the solar radiation is high and the PV capacity cost is down by 50% from \$$4\times10^6$/MW.

The values of parameters used for testing the model are carefully chosen based on the knowledge and information from real applications and related literature. For instance, the parametric data associated with WT and PV systems in Table 3 are derived based on NREL [13], and the wind and solar capacity factors (i.e. H, M, L) are segmented based on the report of Weather Underground [14]. Though variations of power demand exist among manufacturing, warehousing and retailing facilities, the LCOE in each site largely depends on the capacity factor of the onsite generating units, not the actual electric demand. Hence, changes in D_i for i=1, 2, …, 9 will not significant influence the local renewable energy cost.

Table 6: Comparisons under Different Climate Conditions (CF=Capacity Factor)

	Case 1	Case 2	Case 3	Case 4	Case 5	Case 6
Factory CF (WT, PV)	H, H	L, L	L, H	L, H	H, H	H, H
CW CF (WT, PV)	H, H	L, L	L, H	L, H	H, H	L, H
RS CF (WT, PV)	H, H	L, L	L, H	L, H	H, H	L, H
PV Capacity Cost ($/MW)	4×10^6	4×10^6	4×10^6	2×10^6	1×10^6	2×10^6
PV Carbon Credit ($/MWh)	35	35	35	0	0	0
LCOE ($/MWh)	48.35	82.70	82.70	69.07	38.53	64.16
WT Capacity (MW)	170.4	340.8	340.8	0	0	120.4
PV Capacity (MW)	0	0	0	227.23	227.23	106.83

6. Conclusions

This paper presents a simple linear program model to investigate the feasibility of operating a carbon-free supply chain by integrating onsite wind and solar energy. The proposed model is extensively tested under various operating conditions which include high, medium and low wind speed and solar irradiance. The results show that wind generation is cost effective provided a medium wind speed prevails in the local facility. Though PV is less competitive than wind, this technology shows great potential if its cost is reduced by 50%. It is foreseeable that e-freight transportation will play an important role in lowering carbon footprint in logistics network. In the future the current planning model can be expanded by incorporating dynamic utility prices and random climatic conditions under a stochastic programming framework.

References

1. S. Villarreal, J. A. Jimenez, T. Jin, M. Cabrera-Rios, "Designing a sustainable and distributed generation system for semiconductor wafer fabs," IEEE Transactions on Automation Science and Engineering, vol. 10, no. 1, 2013, pp. 10-16.
2. U.S. Transportation GHG Emissions. Available http://www3.epa.gov/otaq/climate/documents/420f13033a.pdf. (accessed on January 3, 2016).
3. Truckinfo, Trucking Statistic, available from: http://www.truckinfo.net/trucking/stats.htm, (accessed on Dec. 17, 2015).
4. D. Ozment, "Walmart's Commitment to Solar," May 09, 2014, available at http://blog.walmart.com/sustainability/20140509/walmarts-commitment-to-solar, (accessed on October 15, 2015).
5. Bakry, T. Attya, T. Hartkopf, "Utilising stored wind energy by hydro-pumped storage to provide frequency support at high levels of wind energy penetration," IET Generation, Transmission & Distribution, 2015, vol. 9, no. 12, pp. 1485-1497.
6. S. Benjaafar, Y., Li, M. Daskin, "Carbon footprint and the management of supply chains: insights from simple models," IEEE Transactions on Automation Science Eng. vol. 10, no. 1, 2013, pp. 99-116.
7. Y.-T. Chen, M.-Ch. Chiu, "A case-based method for service-oriented value chain and sustainable network design," Advanced Engineering Informatics, vol. 29, 2015, pp. 269-294.
8. C.P. Cameron, A.C. Goodrich, "The levelized cost of energy for distributed PV: A parametric study," The 5th IEEE Photovoltaic Specialists Conference, 2010, pp. 529-534 (available from IEEE Xplore database).
9. U.S. Energy Information Administration (EIA), "How much of U.S. carbon dioxide emissions are associated with electricity generation?" <http://www.eia.gov/tools/faqs/faq.cfm?id=77&t=11>, (accessed May 29, 2014).
10. T. Cai, S. Duan, and C. Chen, "Forecasting power output for photovoltaic grid-connected power systems without using solar radiation measurement," in Proceedings of Power Electronics for Distributed Generation Systems Symposium, 2010, pp. 773-777.
11. SAE International, "SAE standard on EV charging connector approved," available at http://www.sae.org/, (accessed on Nov. 11, 2015).
12. Nissan, "2015 Nissan LEAF® Electric Car Specs," 2015, available at http://www.nissanusa.com/electric-cars/leaf/charging-range/battery/ (accessed on October 20, 2015).
13. National Renewable Energy Laboratory (NREL), "Distributed generation renewable energy estimate of costs," 2013, available at http://www.nrel.gov/analysis/tech_lcoe_re_cost_est.html, (accessed May 7, 2015).
14. Weather Underground (WU), 2014, available at http://www.wunderground.com/ (accessed November 10, 2015).